Modeling of Cyclic Shear-Flexure Interaction in Reinforced Concrete Structural Walls. I: Theory

Kristijan Kolozvari, Ph.D.[1]; Kutay Orakcal, Ph.D.[2]; and John W. Wallace, Ph.D., P.E., M.ASCE[3]

Abstract: Existing approaches used to model the lateral load versus deformation responses of reinforced concrete walls typically assume uncoupled axial/flexural and shear responses. A novel analytical model for RC walls that captures interaction between these responses for reversed-cyclic loading conditions is described. The proposed modeling approach incorporates RC panel behavior into a two-dimensional fiber-based macroscopic model. The coupling of axial and shear responses is achieved at the macrofiber (panel) level, which further allows coupling of flexural and shear responses at the model element level. The behavior of RC panel elements under generalized, in-plane, reversed-cyclic loading conditions is described with a constitutive fixed-strut-angle panel model formulation. The sensitivity of model results to various modeling parameters is investigated and results of the sensitivity studies are presented, whereas detailed information on calibration and validation of the proposed modeling approach is presented in a companion paper. **DOI: 10.1061/(ASCE)ST.1943-541X.0001059.**

Author keywords: Reinforced concrete; Structural walls; Analytical modeling; Shear-flexure interaction; Analysis and computation.

Introduction

The role of reinforced concrete (RC) structural walls in buildings is to provide sufficient lateral strength and stiffness to limit nonlinear behavior during service level earthquakes, as well as to provide reliable nonlinear deformation capacity (ductility) during design and maximum considered earthquakes. Wall behavior is generally classified according to wall aspect ratio (h_w/l_w) or shear-span -to-depth ratio (M/Vl_w), as either shear-controlled (walls with aspect ratio less than approximately 1.0–1.5) or flexure-controlled (aspect ratios greater than 2.5–3.0). For walls between these aspect ratios, herein referred to as moderate aspect ratio walls, nonlinear responses associated with both axial/bending and shear behavior are likely; although flexural yielding is expected, nonlinear shear deformations may be significant and lead to reduced lateral stiffness, strength, and ductility.

Experimental results have shown that flexural and shear yielding of moderate aspect ratio walls occur near-simultaneously, even when wall nominal shear strength is as much as twice the shear developed at flexural yielding (Massone and Wallace 2004), suggesting interaction between nonlinear flexural and shear behavior, commonly referred to as shear-flexure interaction (SFI). This interaction has been observed in a number of experimental studies on slender RC walls with aspect ratios greater than 2.0 (e.g., Wang et al. 1975; Vallenas et al. 1979; Oesterle et al. 1976, 1979; Hines et al. 1995, 2002; Thomsen and Wallace 2004; Sayre 2003; Dazio et al. 2009; Lowes et al. 2012), with shear deformations contributing more than 20% to top lateral displacement (Massone and Wallace 2004; Beyer et al. 2011; Lowes et al. 2012). Test results reported by Tran and Wallace (2012) revealed that the degree of interaction increases for moderately slender walls with aspect ratios equal to 1.5 and 2.0, where nonlinear shear deformations constituted as much as 50 and 30% of the wall top displacement, respectively.

Use of element models based on uniaxial material stress versus strain relations; such as available displacement-based and force-based fiber models and the multiple-vertical-line-element-model (MVLEM) (Vulcano 1992; Vulcano et al. 1988; Fischinger et al. 1990; Orakcal et al. 2004) have become very common in both research (OpenSees) (McKenna et al. 2000) and engineering practice (*Perform-3D*). Although these models, as well as the majority of other available analytical models, have been shown to reasonably represent axial-bending behavior of RC walls (Orakcal and Wallace 2006), they usually do not incorporate experimentally observed SFI; the shear behavior of a RC wall is typically described using ad hoc force-deformation rules defined independently from the axial/bending modeling parameters (Vulcano and Bertero 1987; Orakcal et al. 2004). Previous research has shown that analytical predictions obtained using *uncoupled* models may underestimate axial compressive strains even in relatively slender RC walls controlled by flexure (Orakcal and Wallace 2006), and overestimate the lateral load capacity of particularly moderate-aspect-ratio (Tran 2012) and low-aspect-ratio walls (Massone et al. 2006).

Various approaches have been proposed to capture the observed coupling between nonlinear flexural and shear behavior in RC walls. Beyer et al. (2011) proposed an empirical (or semiempirical) approach in which the ratio between flexural and shear deformations depends on wall geometry, axial strain, and crack angle. Although this methodology has been shown to produce a reasonable estimate of the ratio between shear and flexural deformations for walls controlled by flexure, albeit with significant dispersion, the approach is limited due to its reliance on test data (i.e., interpolation and extrapolation without an underlying behavior-based model). A strut-and-tie (truss) approach provides an alternative methodology to capture SFI (Panagiotou et al. 2011) in RC walls and deep beams (Scott et al. 2012a, b). The model by

[1]Senior Engineer/Analyst, Saiful/Bouquet Structural Engineers Inc., Pasadena, CA 91101 (corresponding author). E-mail: kolozvari@yahoo.com

[2]Associate Professor, Dept. of Civil Engineering, Bogazici Univ., Bebek-Istanbul 34342, Turkey. E-mail: kutay.orakcal@boun.edu.tr

[3]Professor, Dept. of Civil and Environmental Engineering, Univ. of California, Los Angeles, CA 90095-1593. E-mail: wallacej@ucla.edu

Note. This manuscript was submitted on May 31, 2013; approved on February 21, 2014; published online on July 18, 2014. Discussion period open until December 18, 2014; separate discussions must be submitted for individual papers. This paper is part of the ***Journal of Structural Engineering***, © ASCE, ISSN 0733-9445/04014135(10)/$25.00.

Panagiotou et al. (2011) accounts for the interaction between shear and flexural responses by reducing the concrete compressive strut capacity as a function of transverse tensile strain. However, due to overlapping areas of vertical, horizontal, and diagonal concrete struts in the model, achieving accurate displacement responses over a broad range of response amplitudes is a challenge, which is a known issue with strut-and-tie models (Ramirez and Breen 1991). The methodology proposed by Petrangeli et al. (1999), which involves implementation of a constitutive RC membrane (panel) model into finite-element formulation of a fiber-based model, is commonly used to incorporate SFI into fiber-based models for structural walls (e.g., Massone et al. 2006, 2009; Fischinger et al. 2012; Jiang and Kurama 2010; Kolozvari et al. 2012). Since the constitutive panel model describes biaxial behavior of concrete, the interaction between axial and shear responses is captured at the constitutive panel level, which in turn allows incorporation of SFI directly at the model element level. Fischinger et al. (2012) presented a multiple spring model based on this methodology to capture SFI by assigning a shear spring, which considers shear resisting mechanisms for aggregate interlock, dowel action, and horizontal reinforcement based on a crack width, to each macro fiber of MVLEM. The uniaxial and shear resisting mechanisms are defined by the use of force-deformation constitutive rules. The model results have been shown to capture test results for a five-story coupled wall tested on a shaking table under biaxial excitation. Although the model seems promising, only limited calibration against dynamic test data has been done, and further model calibration against experimental data for walls with significant SFI is needed. Massone et al. (2006) implemented a rotating-angle softened truss model (Pang and Hsu 1995) into a MVLEM formulation to capture SFI. This approach was shown to reasonably capture SFI in moderate- and low-aspect ratio RC walls; however, the developed model formulation, based on rotating-angle softened truss model, is not easily amenable to cyclic loading.

Overall, modeling approaches available in the literature for representing the experimentally-observed SFI behavior are characterized with four significant shortcomings: (1) models are empirical or have cumbersome formulations, (2) models are capable of simulating monotonic responses only, (3) sensitivity of model results to material and modeling parameters have not been studied in detail, and (4) models have not been sufficiently validated against experimental data at both global (load displacement) and local (rotations, curvatures, strains) response levels, especially for cases where significant interaction is observed.

Given the widespread use of moderate-aspect ratio walls in buildings with 4 to 10 stories, as well as relatively low shear-span-to-depth ratios in core walls of taller buildings, there is a need for relatively simple analytical model that is able to capture the interaction between axial, flexural, and shear responses in RC structural walls under reversed-cyclic loading conditions. In addition, the model needs to be validated against both global and local responses for a range of response amplitudes using data from heavily instrumented tests on moderate-aspect ratio wall specimens. Therefore, a research project was undertaken to develop a novel analytical model for RC walls that captures interaction between nonlinear flexural and shear responses under reversed-cyclic loading conditions, as well as to validate the model against detailed experimental data obtained from tests on RC wall specimens that experienced significant levels of SFI. A description of the proposed model, significant characteristics of the model response predictions, and sensitivity of the model predictions to various modeling parameters are presented in this paper, whereas detailed comparisons with experimental results reported by Tran and Wallace (2012) are provided in the companion paper (Kolozvari et al. 2014).

Analytical Model Formulation

The proposed analytical model incorporates RC panel behavior into a 2D macroscopic fiber model in order to capture SFI in RC walls. In this study, the MVLEM implemented by Orakcal et al. (2004) is chosen as the baseline model for implementation of a new cyclic SFI model because of its relatively simple formulation, numerical stability, efficiency, and reasonably accurate predictions of flexural responses (Orakcal and Wallace 2006). In the original formulation of MVLEM [Fig. 1(a)], shear and flexural deformations are uncoupled and element macrofibers are represented by uniaxial elements whose responses are combined to describe flexural (axial bending or P-M) behavior of the model element. Shear behavior is modeled using a horizontal spring placed at the height ch whose behavior is typically described using nonlinear ad hoc force-deformation rules (e.g., an origin-oriented hysteresis model by Kabeyasawa et al. 1983). In the proposed SFI model formulation, each uniaxial (macrofiber) element from the original formulation of the MVLEM is replaced with a RC panel element subjected to membrane actions [Figs. 1(b and c)]. Behavior of the RC panel elements under reversed cyclic loading conditions is described using a 2D constitutive RC panel model formulation [Fig. 1(b)] based on the fixed-strut-angle-model (FSAM) developed by Ulugtekin (2010) and extended by Orakcal et al. (2012) to incorporate shear aggregate interlock effects. The coupling of axial and shear responses is thus enabled at the panel (macrofiber) level, which further allows coupling of flexural and shear responses at the model element level. Although the approach is conceptually similar to the one proposed by Massone et al. (2006), which

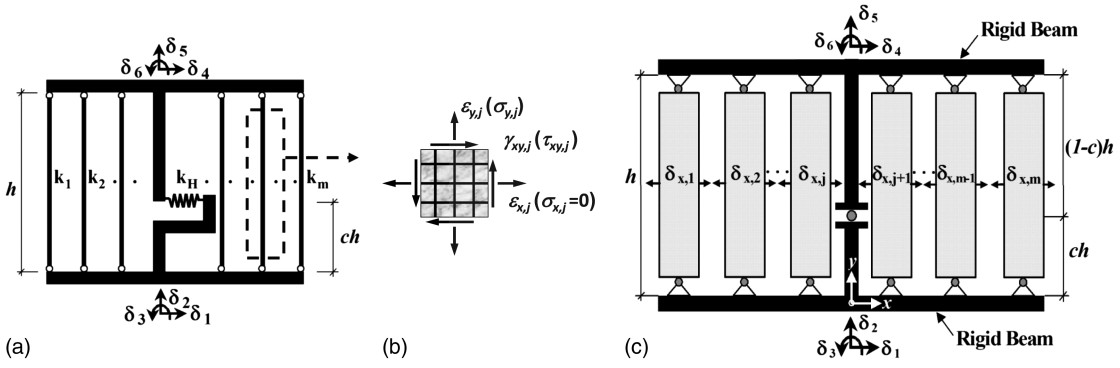

Fig. 1. Element models: (a) original MVLEM element; (b) RC panel element; (c) SFI-MVLEM element

J. Struct. Eng., 2015, 141(5): 04014135

addressed monotonic responses only, the proposed model with the FSAM panel model is capable of simulating cyclic responses.

A structural wall is modeled as a stack of n, 2D, modified MVLEM elements (referred to as SFI-MVLEM elements), with m macrofibers connected to two rigid beams at the top and bottom of each model element. The exterior macrofibers represent the wall boundary elements (where longitudinal reinforcement is typically concentrated), while the interior macrofibers represent the wall web panel between the boundary elements. In the SFI-MVLEM formulation, each macrofiber is a panel element comprising concrete and both vertical and horizontal reinforcement, representing a 2D constitutive behavior that relates average (smeared) axial strains in vertical and horizontal directions ε_x and ε_y and the average shear strain γ_{xy}, with average axial stresses σ_x and σ_y and average shear stress τ_{xy} [Fig. 1(b)]; the average stresses on each panel element are the resultant of the contributions from concrete and reinforcing steel. Similar to the original MVLEM formulation, relative rotation between the top and bottom rigid beams of the wall element are concentrated at relative height ch [Fig. 1(c)]. A value of $c = 0.4$ is adopted in the model formulation as recommended by Vulcano et al. (1988) for flexure and verified by Orakcal and Wallace (2006). Rotations and resulting lateral displacements are obtained based on the wall curvature and shear deformations developing on each model element, corresponding to the imposed bending moment and shear force.

In the model formulation, the longitudinal normal (axial) strain ε_y and shear strain γ_{xy} values are initially calculated for the entire wall cross section (for all panel macrofibers) based on the six prescribed degrees of freedom defined at the top and bottom of the model element $\{\delta_N\} = \{\delta_1 \delta_2, \ldots, \delta_6\}^T$ [Fig. 1(c)], based on the assumptions that plane-sections-remain-plane after loading and shear strains along the wall section are uniformly distributed. Horizontal normal strain ε_x on each RC panel element [necessary to complete the strain field in each panel, Fig. 1(b)], is defined by the use of additional degrees of freedom in the horizontal direction $\{\delta_x\} = \{\delta_{x,1} \delta_{x,2}, \ldots, \delta_{x,m}\}^T$ as shown on Fig. 1(c). These horizontal (extensional) degrees of freedom on the panel macrofibers are assumed to be kinematically independent from the six nodal displacement degrees of freedom at the top and bottom of the element; therefore, the total degrees of freedom necessary to describe the deformation of one SFI-MVLEM element is increased, from six in the original formulation of the MVLEM, to $6 + m$.

For any level of deformation (strain field) imposed on each RC panel, described by three strain degrees of freedom ε_x, ε_y and γ_{xy}, the stiffness properties and force-deformation relationships of the panel macrofibers are defined according to the implemented constitutive panel model and the tributary areas of concrete and reinforcing steel assigned to each panel macrofiber. The model element stiffness matrix given by Eq. (1) is a combined matrix consisting of two submatrices $[K_e]^N$ and $[K_e]^x$, since the displacements along six nodal degrees of freedom $\{\delta_N\}$ and m extensional degrees of freedom $\{\delta_x\}$ are assumed to be kinematically independent

$$[K_e] = \begin{bmatrix} [K_e]^N & [0] \\ [0] & [K_e]^x \end{bmatrix} \tag{1}$$

Submatrix $[K_e]^N$ is the element stiffness matrix relative to the six nodal degrees of freedom $\{\delta_N\}$ as described by Orakcal et al. (2004), while the submatrix $[K_e]^x$ is the element stiffness matrix corresponding to the m extensional degrees of freedom $\{\delta_x\}$, and is expressed as a diagonal matrix

$$[K_e]^x = \text{diag}\{\, k_{x,1} \quad k_{x,2} \quad , \ldots, \quad k_{x,m} \,\} \tag{2}$$

Similarly, the corresponding internal force vector of the model element can be written as

$$\{F_{e,\text{int}}\} = \begin{Bmatrix} \{F_{e,\text{int}}\}^N \\ \{F_{e,\text{int}}\}^x \end{Bmatrix} \tag{3}$$

where $\{F_{e,\text{int}}\}^N$ = element force vector relative to the six nodal displacement degrees of freedom $\{\delta_N\}$; $\{F_{e,\text{int}}\}^x$ = element force vector corresponding to the m extensional degrees of freedom $\{\delta_x\}$. The element force subvector $\{F_{e,\text{int}}\}^N$ is derived from the resulting axial forces in vertical direction ($F_{y,j}$) and shear forces ($F_{xy,j}$) in jth macrofiber [RC panel, Fig. 1(c)], as derived by Orakcal et al. (2004) for the original MVLEM formulation, while the element force subvector $\{F_{e,\text{int}}\}^x$ relative to the extensional degrees of freedom $\{\delta_x\}$ is given by

$$\{F_{e,\text{int}}\}^x = \{\, F_{x,1} \quad F_{x,2} \quad , \ldots, \quad F_{x,m} \,\}^T \tag{4}$$

where $F_{x,j}$ $(j = 1, \ldots, m)$ = force in the x direction at jth RC panel.

Since vertical faces of RC panels of one model element are not in contact with each other, additional constraints are needed in horizontal x direction to complete the strain field on each panel. In the model formulation presented here, the resultant transverse normal stress σ_x within each panel macrofiber (resultant of the contributions from concrete and reinforcing steel) is assumed to be zero, which is consistent with the boundary conditions with no transverse loads applied over the wall height (except at the top). Previous studies conducted by Massone et al. (2009) revealed that the zero resultant horizontal stress assumption is not capable of correctly reproducing experimental responses observed in walls with low shear span-to-depth ratios (lower than approximately 1.0), underestimating the lateral load capacity of the wall by 13–40%. Therefore, given the assumption of zero resultant stress along the length of the wall ($\sigma_x = 0$), application of the proposed model formulation is not recommended for walls with aspect ratios greater than 1.0. This study focuses on the application of the proposed modeling approach to walls with aspect ratios between 1.0 and 3.0, for which significant SFI is expected. In order to simulate the response of squat walls with aspect ratios less than 1.0, for which nonlinear shear behavior is expected to dominate the response, use of an empirical relationship to describe the distribution of average transverse normal strains (ε_x) over the wall height (e.g., as proposed by Massone et al. 2009) could be implemented in the model formulation.

RC Panel Behavior

The constitutive RC panel behavior under generalized reversed-cyclic in-plane actions is described by the FSAM developed by Ulugtekin (2010) and extended by Orakcal et al. (2012) to incorporate shear aggregate interlock effects. The formulation of the FSAM model is based on the concept of smeared stresses and involves several assumptions: the assumption of a perfect bond between concrete and reinforcing steel bars (i.e., the proposed model formulation does not consider the effect of bond-slip deformations and bond stresses on predicted model responses), the assumption of zero reinforcement dowel action, and the assumption that the direction of concrete compression struts coincide with the directions of concrete cracks. Biaxial stress-strain relationships are

used to represent the behavior of concrete along compression struts, the orientation of which remain unchanged after cracking occurs, while the behavior of reinforcing steel is described by uniaxial stress-strain relationships applied along the directions of reinforcing steel bars.

The formulation of the constitutive panel model is characterized by three stages of RC panel behavior: (1) uncracked concrete, (2) behavior after formation of the first crack, and (3) behavior after formation of the second crack. The initial (uncracked) stage of concrete behavior [Fig. 2(a)] under cyclic loading is represented with a rotating angle approach [similar to the modified compression field theory, Vecchio and Collins (1986), and the rotating angle-softened truss model, Pang and Hsu (1995)], assuming that the concrete principal stress and strain directions coincide (and rotate) and concrete behavior is represented by a monotonic stress-strain relationship, which has been shown to be reasonable for the uncracked stage of concrete behavior only. The first crack is assumed to form when the value of the principal tensile strain in concrete exceeds a specified cracking strain of concrete; the model records the principal strain direction corresponding to first cracking of concrete (referred to as the first *fixed strut* direction). The generalized strain field acting on concrete is transformed to fixed directions along and perpendicular to the first *fixed strut* direction, along which biaxial stress-strain relationships for concrete are applied [Fig. 2(b)]. The second crack is formed when the strain along the first strut direction first exceeds the cracking strain. It is assumed that the second crack (second *fixed strut*) will develop perpendicular to the direction of the first crack. For further loading stages, the generalized strain field acting on concrete is transformed into strains along the first and second fixed strut directions, along which the biaxial hysteretic stress-strain relationships for concrete are applied [Fig. 2(c)]. Details of the FSAM formulation are available in the thesis by Ulugtekin (2010).

The main inherent assumption in the formulation of the FSAM is that the principal stress directions in concrete coincide with crack directions, suggesting that the shear stresses developed along crack surfaces due to shear strains associated with sliding along cracks have marginal influence on the RC panel behavior (Stevens et al. 1991), and thus, are ignored. However, it has been observed that the zero-aggregate interlock assumption may result in overestimation of sliding shear strains along crack surfaces for panels with nonequal reinforcement ratios in x and y directions (Orakcal et al. 2012), which may lead to overestimation of shear deformations in RC walls and underestimation of wall strength (Kolozvari 2013). Therefore, prior to implementation in the SFI-MVLEM, the original FSAM formulation was modified to represent shear resisting mechanisms along cracks, as described in the following section.

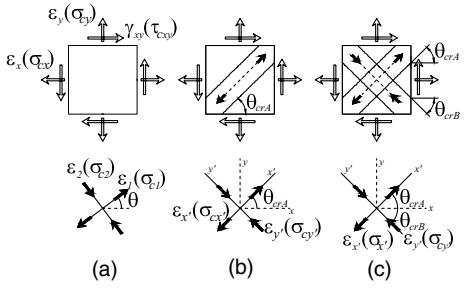

Fig. 2. Concrete biaxial behavior in the FSAM: (a) uncracked behavior; (b) behavior after formation of first crack; (c) behavior after formation of second crack

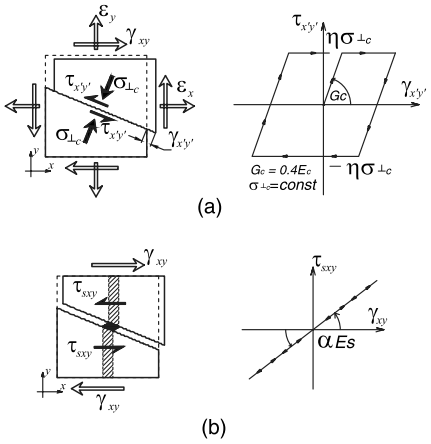

Fig. 3. Shear resisting mechanisms along the cracks of RC panel element: (a) shear aggregate interlock model; (b) dowel action model

Modeling of Shear Resisting Mechanisms

The mechanism that transfers shear force across cracks in a RC panel consists of interlock of aggregate protrusions on the crack surfaces (shear aggregate interlock) and dowel action of reinforcing bars. The shear aggregate interlock effects are represented by the simple friction-based cyclic modeling approach (Orakcal et al. 2012) shown in Fig. 3(a). The shear stress-strain relationship along the crack starts with linear loading/unloading behavior with slope of $0.4E_c$ (representing the elastic shear modulus of concrete), relating sliding shear strain along a crack to shear stress via a linear elastic relationship between the sliding shear strain and the resultant shear stress along the crack surface. The shear stress is restrained to zero value when the concrete normal stress perpendicular to the crack is tensile (crack open) and is bounded by the product of a shear friction coefficient η and the concrete normal stress perpendicular to the crack $\sigma_{\perp c}$, when the concrete normal stress is compressive (crack closed). Under constant concrete compressive stress perpendicular to the crack ($\sigma_{\perp c}$ = const), this model yields an elastoplastic aggregate interlock behavior under cyclic loading, as shown on Fig. 3(a).

Implementation of the RC panel model with the described shear aggregate interlock model alone resulted in analytical predictions in which pinching attributes of the force-deformation response were overestimated due to zero shear stiffness along open cracks at low lateral load levels. Since dowel action on reinforcing bars can provide shear resistance along cracks, even when the crack is open and as long as the crack width is small, a simple linear-elastic constitutive model is implemented in RC panel model to simulate the contribution of reinforcement to the shear transfer mechanism along a crack. In the present model, it is assumed that the shear resisting dowel mechanism acts in the horizontal plane of the wall. The relationship between shear strain acting on a panel element in the horizontal plane of the wall (γ_{xy}) and the resulting shear stress on vertical reinforcing steel bars (τ_{sxy}) is described by

$$\tau_{sxy} = \alpha \cdot E_s \cdot \gamma_{xy} \tag{5}$$

where E_s = elastic steel (Young's) modulus; α = coefficient [Fig. 3(b)]. Calibration studies to assess appropriate values of α are presented in Kolozvari (2013) and in a companion paper (Kolozvari et al. 2014). This simple behavioral model is only intended to represent the stiffness contribution of reinforcing bars to the shear resistance along a crack surface, with no consideration of the crack width or the longitudinal stresses developing in the

reinforcing bars. When the crack is closed, shear aggregate interlock effects in concrete typically dominate over this dowel effect. As such, contribution of the reinforcing bars to the shear transfer mechanism across the cracks is considered using a very simple behavioral approach in the current model formulation. Alternative models for shear resistance of reinforcement along a crack can be found in the literature (e.g., Dulacska 1972; Vecchio and Lai 2004); implementation of such behavioral models and validation against experimental data can be considered as potential model improvements.

Material Constitutive Models

Since the implemented constitutive RC panel model relates the panel response directly to uniaxial constitutive stress-strain behavior of concrete and reinforcing steel, advanced state-of-the-art hysteretic material constitutive relationships were implemented in the model formulation.

The implemented uniaxial constitutive stress-strain relationship for reinforcing steel is the well-known nonlinear hysteretic model of Menegotto and Pinto (1973), extended by Filippou et al. (1983) to include isotropic strain hardening effects. The model is simple in its formulation and computationally efficient, yet is capable of reproducing experimental results with reasonable accuracy. It captures important behavioral features of the hysteretic behavior of reinforcing steel bars, including Bauschinger's effect, and kinematic and isotropic strain hardening. The stress-strain relationship implemented for reinforcing steel, with the model parameters, is presented on Fig. 4.

The constitutive relationship proposed by Chang and Mander (1994) was implemented to simulate the uniaxial hysteretic behavior of concrete along the *fixed struts*. This model is a relatively complex, rule-based, generalized, and nondimensional constitutive model that allows calibration of the monotonic and hysteretic material modeling parameters, and can simulate the hysteretic behavior of confined and unconfined, ordinary and high-strength concrete, in both cyclic compression and tension (Fig. 5). The model addresses important behavioral features, such as continuous hysteretic behavior under cyclic compression and tension, progressive stiffness degradation associated with smooth unloading and reloading curves at increasing strain values, and gradual crack closure effects. In the panel model formulation implemented here, the original formulation of the Chang and Mander (1994) model is modified to represent behavioral features of concrete under

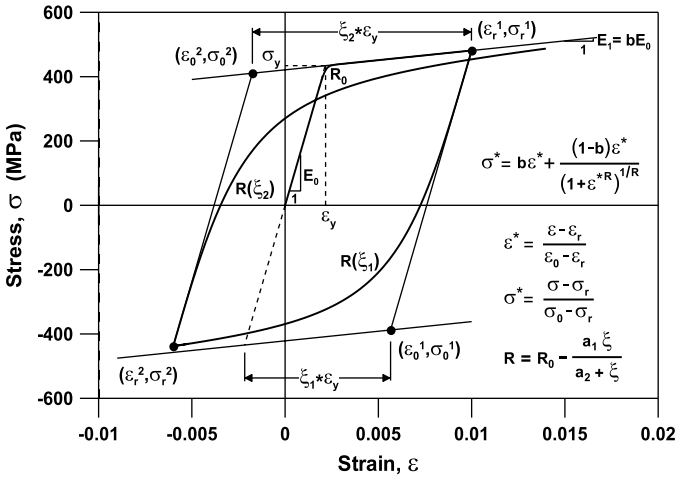

Fig. 4. Uniaxial, cyclic constitutive model for reinforcing steel

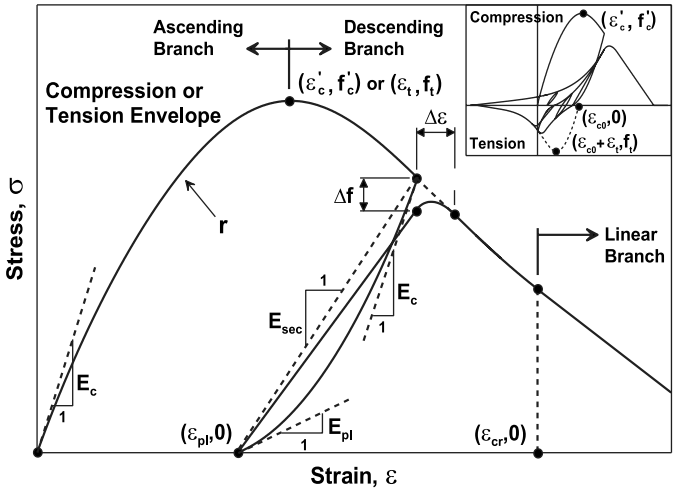

Fig. 5. Uniaxial, cyclic constitutive model for concrete

biaxial loading by including parameters representing compression softening (defined by Vecchio and Collins 1993), hysteretic biaxial damage (defined by Mansour et al. 2002), and tension stiffening effects (defined by Belarbi and Hsu 1994). Kolozvari (2013) and Ulugtekin (2010) provide details on these behavioral features and parameters.

Analysis Results and Parametric Sensitivity Studies

A direct stiffness assembly procedure is used to assemble the SFI-MVLEM elements presented here into a complete wall model, and an incremental-iterative numerical scheme (Clarke and Hancock 1990) is used to perform nonlinear quasistatic analysis of the complete wall model using *Matlab*. Characteristic features of model predictions, sensitivity of the model results to geometric and reinforcement characteristics of a wall (including aspect ratio and web reinforcement ratio), as well as sensitivity of the model results to model parameter (including friction coefficient η, dowel stiffness αE_s, and model discretization) are presented in terms of overall load-deformation response predictions and relative contributions of shear and flexural deformations to the overall response. The objective here is not to present detailed calibration studies against test data, but instead to demonstrate that the model is capable of capturing important response features for walls with various modes of behavior and failure modes, and to assess the sensitivity of model results to variation in model parameters. Detailed comparisons of model and test results are presented in the companion paper (Kolozvari et al. 2014). The cantilever wall specimens tested by Tran and Wallace (2012) that include five test specimens with different aspect ratios, levels of axial load, and quantities of boundary longitudinal, boundary transverse, and web vertical and horizontal reinforcement are used for this purpose.

To provide context to the sensitivity studies presented, specimen RW-A15-P10-S78 tested by Tran and Wallace (2012), is used in this study to assess model capabilities and sensitivity to mentioned parameters. Test specimen RW-A15-P10-S78 had rectangular cross section (RW), aspect ratio of 1.5 (A15) with height of 1,830 mm and length of 1,220 mm, thickness of 152 mm, applied constant axial load of approximately 10% of the design axial load capacity of the wall specimen (P10), designed web shear stress of $0.65\sqrt{f_c'}$ MPa ($7.8\sqrt{f_c'}$ psi, S78; f_c' is the compressive strength of concrete), web reinforcing ratios of 0.73%, and boundary longitudinal reinforcing ratio of 6.06%, resulting in a shear demand at

nominal moment capacity ($V@M_n$) corresponding to 85% of the nominal shear capacity (V_n). The behavior of the specimen was characterized by significant contribution of nonlinear shear deformations, up to 35% of total top lateral deformations, and SFI. The analysis results were obtained using five SFI-MVLEM elements along the height of the wall and five RC panel elements (macrofibers) along the wall length; two external RC panels represented the wall boundary elements with both confined and unconfined (cover) concrete, and three internal RC panels represented the wall web with unconfined concrete. A cyclic displacement history with a target drift level of 3.0%, similar to one used in the test program, is applied at the top of the wall for the analysis; one loading cycle for each drift level of 0.1, 0.25, 0.5, 0.75, 1.0, 1.5, 2.0, and 3.0% is used in the analysis, as opposed to multiple loading cycles applied during the experiment.

Model Response Characteristics

Analytical prediction of the lateral load versus wall top displacement response is presented in Fig. 6. It can be observed from the figure that characteristics of the overall cyclic wall behavior are clearly reflected by the model, including the overall hysteretic shape of the lateral load versus top displacement behavior, degradation of unloading/reloading stiffness, plastic (residual) displacements at zero load level, and moderate pinching behavior. As also shown on Fig. 6, the model predicts a reasonable cracking pattern on the wall, with near-horizontal (flexural) cracks at the wall boundaries and inclined (shear) cracks towards the wall center. Analytical results presented in Figs. 7(a and b) show corresponding lateral load versus shear and flexural deformation components of the top displacement, respectively, indicating that model can successfully capture nonlinear shear and flexural deformations, as well as their coupling through the entire cyclic loading history; flexural and shear yielding occur near simultaneously, at lateral load of approximately 700 kN. It can be also observed from Fig. 7 that the shape of hysteretic loops for flexural behavior show no pinching behavior, whereas hysteretic response in shear is characterized by highly pinched behavior, indicating that the pinching behavior observed in overall load-displacement response is associated with shear behavior. In addition, Fig. 7(a) depicts the relative contributions of shear deformations (average of positive and negative loading cycles) along the wall height at lateral drift levels of 1.0, 2.0, and 3.0%. Predicted contributions of shear deformation to the total lateral displacement range from 45% at the top of the wall to 85% at the wall bottom, indicating larger nonlinear shear deformations at the bottom of the wall where nonlinear flexural deformations are concentrated. Similarly, Fig. 7(b) shows the contribution of flexural deformations to the total lateral top displacement at peak drift levels, revealing that top flexural deformations contribute approximately 55% of the total deformations at all applied drift levels.

Fig. 8 shows the distribution of average vertical normal strains and average shear stresses in unconfined concrete along the wall length at the bottom of the wall at peak drift levels of 0.5, 1.0, 2.0, and 3.0%. It can be observed from Fig. 8 that the neutral axis depth does not significantly change with increasing drift ratios, and that the shear force on the wall is resisted primarily by the concrete panels subjected to vertical (axial/flexural) compressive strain, whereas panels under vertical tensile strain resist very low or no shear stress, demonstrating the interaction between axial (flexural) and shear responses at the element level of SFI-MVLEM. Results presented in Fig. 8 also indicate that at drift levels of 0.5 and 1.0%, panels subjected to higher levels of vertical compression develop higher shear stresses, whereas at a drift level of 2.0% the shear stress at the wall boundary decreases, due to degradation in concrete stresses associated with crushing of unconfined concrete in

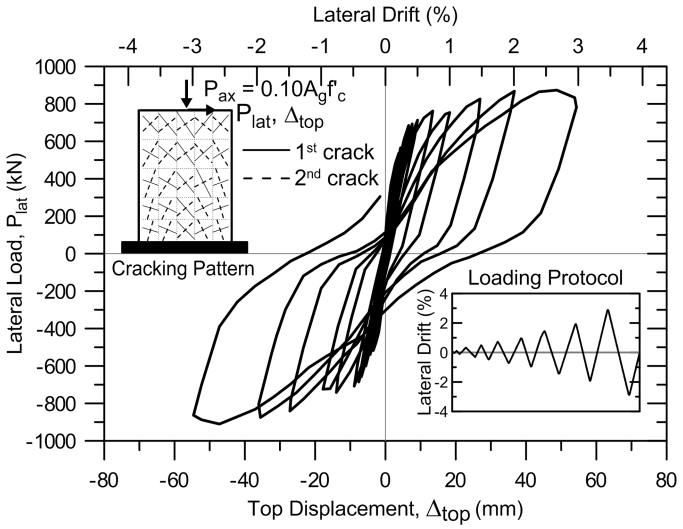

Fig. 6. Lateral load versus top wall displacement predicted by the model

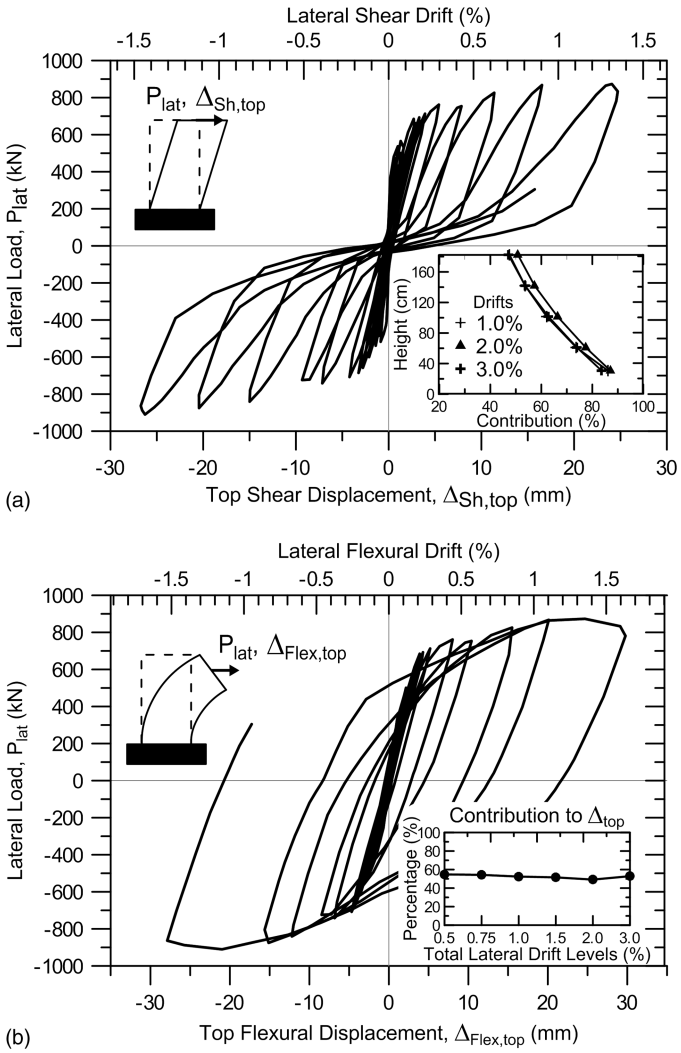

Fig. 7. Load-displacement response predicted by the model: (a) shear; (b) flexure

J. Struct. Eng., 2015, 141(5): 04014135

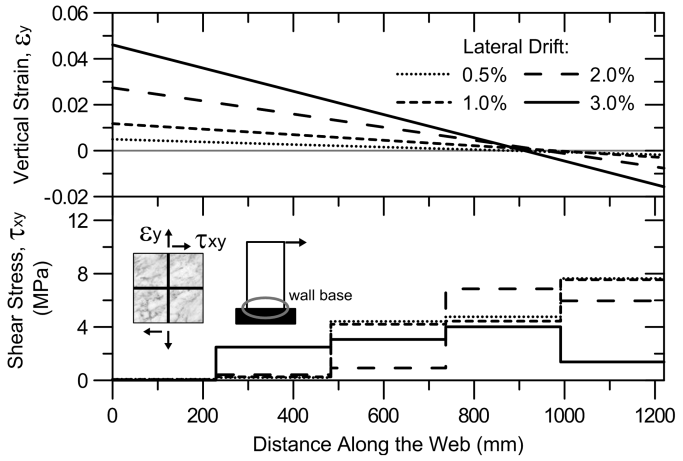

Fig. 8. Vertical strain profiles and distribution of shear stress along the length of the wall

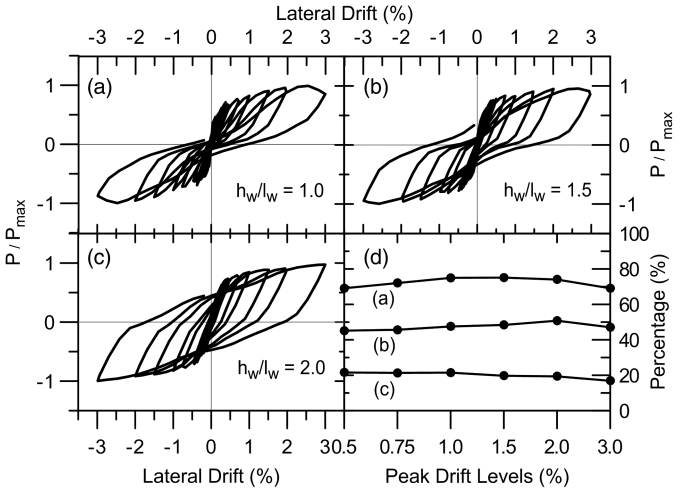

Fig. 9. Sensitivity of model response to wall aspect ratio: (a) $h_w/l_w = 1.0$; (b) $h_w/l_w = 1.5$; (c) $h_w/l_w = 2.0$; (d) contribution of shear deformations to lateral top displacement

the boundary zone. Furthermore, at the drift level of 3.0%, the shear stress migrates from the wall boundary to the web due to further degradation in the stress-strain behavior of the concrete fibers representing the wall cross section at the wall boundary. Overall, Fig. 8 illustrates that the SFI-MVLEM initially imposes more shear stress demand on the boundary zone in compression, and the shear stresses migrate towards the wall web as the concrete compressive stress capacity at the wall boundary degrades.

Sensitivity of Model Response to Wall Configurations

In order to investigate the sensitivity of model predictions to wall aspect ratio, the wall configuration used for previous analyses (representing specimen RW-A15-P10-S78, with aspect ratio of 1.5) was *elongated* to an aspect ratio of 2.0, and *shortened* to an aspect ratio of 1.0, keeping the same cross-sectional dimensions and reinforcement quantities and configurations. Each wall configuration was analyzed under cyclic loading at the top of the wall, to peak drift levels of 0.25, 0.5, 0.75, 1.0, 1.5, 2.0, and 3.0%. Model results obtained for the three cases considered (aspect ratio of 1.0, 1.5, and 2.0) are compared in Fig. 9. The responses obtained for the three aspect ratios can be distinguished by the lateral load capacity prediction, the shape of the overall lateral load versus top displacement response, and the contribution of shear deformation to wall top displacement. For the short wall [aspect ratio of 1.0, Fig. 9(a)], the overall lateral load versus displacement response is characterized with shear-dominated (pinched) hysteretic loops, similar in shape to the pure shear response shown previously in Fig. 7(a), which is consistent with the large contribution of shear deformation to wall lateral displacements, which is more than 70% as shown in Fig. 9(d). In contrast, for the more slender wall [aspect ratio of 2.0, Fig. 9(c)], the shape of the overall response shows wide hysteretic loops and almost no pinching, similar to the shape of the flexural load-displacement response shown on Fig. 7(b), indicating that flexural deformation contributes significantly to lateral displacements, and the contribution of shear deformations is small [limited to approximately 20%, as shown in Fig. 9(d)]. The predicted response of the wall with the intermediate aspect ratio of 1.5 [original specimen, Fig. 9(b)] falls between the walls with aspect ratios of 1.0 and 2.0 in terms of the pinching characteristics of the response and contribution of shear deformations to wall lateral displacements, as moderately pinched hysteresis loops are obtained and the contribution of shear deformations is approximately 45% [Fig. 9(d)]. Furthermore, as expected, the lateral load capacities predicted for the three walls decrease with increasing aspect ratio.

The sensitivity of the model response to the web reinforcement ratio (ρ_{web}) of the wall also was investigated in order to evaluate whether the model can capture variations in behavior associated with changes in the relative contributions of flexural and shear deformations due to changes in the relative wall nominal flexural and shear capacities. For this purpose, the wall web reinforcement ratios were reduced to half of its original values (from 0.73 to 0.36%) for both web vertical and horizontal reinforcement. The original wall specimen had nominal flexural lateral load capacity of 809 kN and nominal shear capacity of 947 kN, resulting in a shear demand at nominal flexural capacity ($V@M_n$) corresponding to 85% of the nominal shear capacity (V_n). When the web reinforcement ratio is reduced to half, the nominal flexural lateral load capacity of the wall decreases to 761 kN, whereas the nominal shear capacity decreases to 645 kN, resulting in shear demand at nominal flexural capacity ($V@M_n$) corresponding to 118% of the nominal shear capacity (V_n). Fig. 10 depicts the lateral load versus top

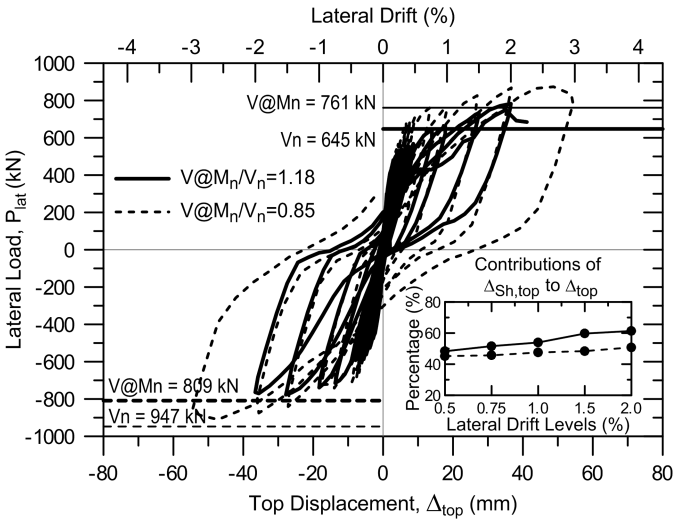

Fig. 10. Sensitivity of model response to web reinforcement ratio

displacement responses obtained for the original wall and the wall configuration with reduced web reinforcement, as well as contributions of shear deformation to the lateral displacement at the top of each wall. It can be observed from the figure that when the flexural capacity of the wall is lower than its nominal shear capacity ($V@M_n/V_n = 0.85$), the model predicts a more flexure-dominated behavior, characterized by only moderate pinching in load-displacement response, and shear deformations contributing approximately 45% to wall lateral displacement. In contrast, when the flexural capacity of the wall is higher than its nominal shear capacity ($V@M_n/V_n = 1.18$), the model predicts a more shear-dominated behavior, with more pinched load-displacement loops, higher contribution of shear deformations (approximately 55% of wall top lateral displacement), and reduced ductility characteristics due to initiation of degradation in the load-displacement response before reaching the target drift level of 3.0%, For both cases, the model yields a lateral load capacity which is slightly larger (approximately 15%) than the *controlling* capacity of the wall (smaller of nominal flexural and nominal shear capacities).

Sensitivity of Model Response to Model Parameters

Apart from parameters associated with the material constitutive models, the user-defined parameters of the model include: the number of RC panel elements used along the length of the wall cross section (m), the number of SFI-MVLEM elements stacked on top of each other along the height of the wall (n), the parameter defining the location of the centroid of rotation along the height of each SFI-MVLEM element (c), the friction coefficient of the shear aggregate interlock (η), and stiffness of shear resisting mechanism provided by reinforcement (αE_s).

Model predictions obtained using values of aggregate interlock friction coefficient η of 1.0 and 1.5, as well as using values of dowel coefficient α of 0.005 and 0.01, are compared on Fig. 11, where lateral load versus total top lateral displacement responses are presented, together with contributions of shear deformation to top displacement at increasing drift levels. Results presented in the figure indicate that the predicted overall load-displacement behavior is not very sensitive to the values of friction coefficient or dowel coefficient, in terms of stiffness and lateral load capacity, while pinching behavior is less pronounced with a higher value for coefficient α. Results presented in Fig. 11 also show that the contributions of

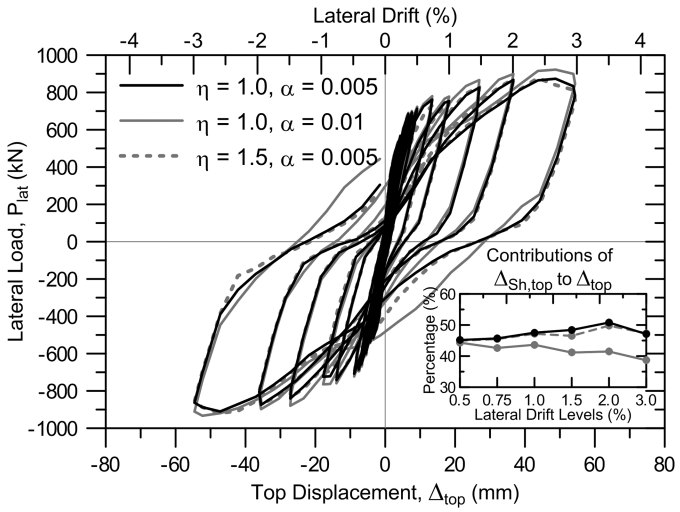

Fig. 11. Sensitivity of model response to parameters of shear aggregate interlock and dowel action

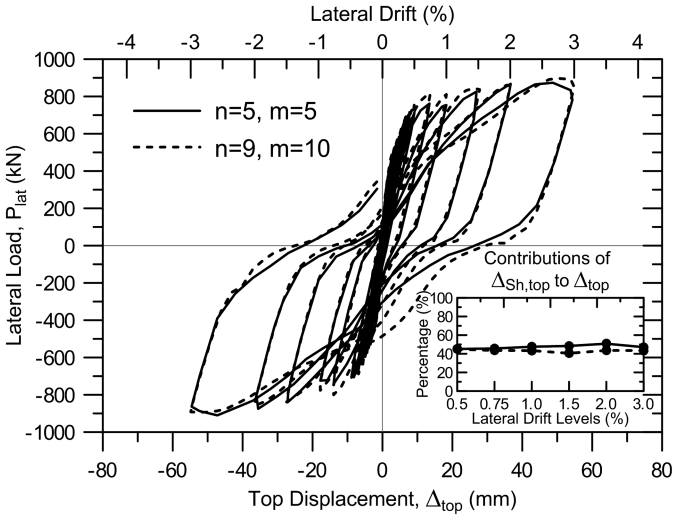

Fig. 12. Sensitivity of model responses to wall discretization

nonlinear shear deformations to top displacement are slightly less for higher values of friction coefficient η, (range from 45% at low drift levels to 50% at higher drift levels), whereas shear deformation contributions are considerably lower for the analysis with higher friction coefficient (about 43% for all drift levels). These results suggest that model predictions are more sensitive to the dowel action stiffness coefficient α than to the shear friction coefficient η in terms of load-deformation response and the contribution of shear deformations. Overall, increasing the shear resistance along the cracks (shear stress) in RC panels, which can be achieved either by increasing the dowel action stiffness coefficient (to a greater extent) or the shear friction coefficient (to a lower extent), results in decrease in the magnitude of shear deformations and shear slip along the cracks of RC panels predicted by the model and also results in less pinching in the overall load-deformation response.

The sensitivity of the simulated wall response to variations of the number of SFI-MVLEM elements along the wall height (n) and the number of RC panel macrofibers along the wall length (m) was also investigated. Fig. 12 shows a comparison of the lateral load-top displacement responses predicted by using either five SFI-MVLEM elements along the wall height with five RC panel elements along the wall length, or by using nine elements along the wall height with 10 RC panel elements along the wall length. The comparison indicates that increasing the number of RC panel elements or the number of SFI-MVLEM elements does not change significantly the prediction of the lateral load versus top displacement relation and contributions of shear deformations to the total lateral displacement at the top of the wall. For prediction of degrading responses, in order to avoid the problem of strain localization, which can occur in displacement-based beam-column elements with distributed plasticity and strain softening material laws (similar to the SFI-MVLEM element), the *regularization* methodology proposed by Coleman and Spacone (2001) can be incorporated to calibrate the model stress-strain relationships, as described by Kolozvari (2013).

Summary and Conclusions

An analytical model that couples wall flexural and shear responses under cyclic loading is proposed. The model incorporates a RC panel behavior described by a fixed-crack-angle approach, into the fiber-based MVLEM. Biaxial stress-strain relationships are used to

J. Struct. Eng., 2015, 141(5): 04014135

represent the behavior of concrete along the compression struts, the orientation of which remain unchanged after cracking occurs, while the behavior of reinforcing steel is described by uniaxial stress-strain relationships applied along the directions of reinforcing steel bars. Simple friction-based shear aggregate interlock model and a linear-elastic model describing shear resistance of reinforcing bars models shear resistance in the RC panel behavior. The variation of model parameters was investigated to identify the sensitivity of analytically predicted wall responses to changes in these parameters. Calibration and validation studies are presented in the companion paper.

Based on analysis results, it was verified that the proposed analytical model captures nonlinear shear deformations and their coupling with nonlinear flexural deformations under cyclic loading conditions throughout the entire loading history. In addition, it was shown that the model successfully captures the hysteretic characteristics of the overall load-displacement response of a wall, systematic tendencies in the contribution of shear and flexural deformations to lateral displacements at different locations on a wall, as well as changes in behavior modes (flexure- or shear-dominant), response characteristics, and lateral load capacity for walls with different aspect ratios, and different shear demands at flexural capacity. Investigation of the sensitivity of analytical results to parameters that contribute to shear resisting mechanisms in RC panel model revealed that the predicted load versus top lateral displacement responses and contributions of shear deformations to the total lateral displacement are not very sensitive to friction coefficient of shear aggregate interlock η, whereas the pinching in load-deformation behavior and the contributions of shear deformations generally increase as the parameter α decreases; doubling the value of parameter α (from 0.005 to 0.01) decreases the contribution of shear deformations by roughly 15% (from approximately 48 to 43%). Furthermore, the predicted wall load-displacement response was shown to be insensitive to model discretization.

Overall, the macroscopic wall model presented herein provides a flexible platform to assess nonlinear cyclic response for RC walls by incorporating interaction between nonlinear shear and flexural responses. Potential model improvements include improvement of the $\sigma_x = 0$ assumption enforced on each macrofiber, to allow extension of the model to lower aspect wall ratios, and consideration of alternative (simple) constitutive models capable of providing a more realistic representation of shear resisting mechanisms across a crack. The model formulation also can be extended to simulate the response of flanged walls under bidirectional loading, although only the in-plane shear stiffness and shear behavior of the constitutive panel elements would be represented along the wall flange or wall web directions. The model is being implemented into OpenSees (McKenna et al. 2000), a widely-used computational platform, to provide improved analytical capabilities for assessing the behavior of RC wall buildings under earthquake excitations, which is essential for application of performance-based seismic design.

Acknowledgments

The work presented in this paper was supported by funds from the National Science Foundation under Grants CMMI-0825347 and CMMI-1208192, as well as the funds provided by the National Science Foundation under Grant No. 0963183, which is an award funded under the American Recovery and Reinvestment Act of 2009 (ARRA). Any opinions, findings, and conclusions expressed in this paper are those of the authors and do not necessarily reflect those of the supporting organizations acknowledged herein.

References

Belarbi, A., and Hsu, T. C. (1994). "Constitutive laws of concrete in tension and reinforcing bars stiffened by concrete." *ACI Struct. J.*, 91(4), 465–474.

Beyer, K., Dazio, A., and Pristely, M. J. N. (2011). "Shear deformations of slender reinforced concrete walls under seismic loading." *ACI Struct. J.*, 108(2), 167–177.

Chang, G. A., and Mander, J. B. (1994). "Seismic energy based fatigue damage analysis of bridge columns: Part I—Evaluation of seismic capacity." *NCEER Technical Rep. No. NCEER-94-0006*, State Univ. of New York, Buffalo, NY, 222.

Clarke, M. J., and Hancock, G. J. (1990). "A study of incremental-iterative strategies for non-linear analyses." *Int. J. Numer. Methods Eng.*, 29(7), 1365–1391.

Coleman, J., and Spacone, E. (2001). "Localization issues in forced-based frame elements." *J. Struct. Eng.*, 10.1061/(ASCE)0733-9445(2001)127:11(1257), 1257–1265.

Dazio, A., Beyer, K., and Bachmann, H. (2009). "Quasi-static cyclic tests and plastic hinge analysis of RC structural walls." *Eng. Struct.*, 31(7), 1556–1571.

Dulacska, H. (1972). "Dowel action of reinforcement crossing cracks in concrete." *ACI Struct. J.*, 69(12), 754–757.

Filippou, F. C., Popov, E. G., and Bertero, V. V. (1983). "Effects of bond deterioration on hysteretic behavior of reinforced concrete joints." *EERC Rep. No. UCB/EERC-83/19*, Earthquake Engineering Research Center, Univ. of California, Berkeley, CA, 184.

Fischinger, M., Rejec, K., and Isaković, T. (2012). "Modeling inelastic shear response of RC walls." *Proc., 15th World Conf. on Earthquake Engineering*, Lisbon, Portugal.

Fischinger, M., Vidic, T., Selih, J., Fajfar, P., Zhang, H. Y., and Damjanic, F. B. (1990). "Validation of a macroscopic model for cyclic response prediction of RC walls." *Computer Aided Analysis and Design of Concrete Structures*, N. B. Bicanic and H. Mang, eds., Vol. 2, Pineridge Press, Swansea, 1131–1142.

Hines, E. M., Dazio, A., and Seible, F. (2002). "Seismic performance of hollow rectangular reinforced concrete piers with highly-confined boundary elements phase III: Web crushing tests." *Rep. No. SSRP-2001/27*, Univ. of California, San Diego, 239.

Hines, E. M., Seible, F., and Priestley, M. J. N. (1995). "Cyclic tests of structural walls with highly-confined boundary elements." *Rep. No. SSRP-99/15*, Univ. of California, San Diego, 266.

Jiang, H., and Kurama, Y. C. (2010). "Analytical modeling of medium-rise reinforced concrete shear walls." *ACI Struct. J.*, 107(4), 400–410.

Kabeyasawa, T., Shiohara, H., Otani, S., and Aoyama, H. (1983). "Analysis of the full-scale seven-story reinforced concrete test structure." *J. Faculty Eng.*, 37(2), 432–478.

Kolozvari, K. (2013). "Analytical modeling of cyclic shear—Flexure interaction in reinforced concrete structural walls." Ph.D. dissertation, Univ. of California, Los Angeles.

Kolozvari, K., Tran, T., Wallace, J. W., and Orakcal, K. (2012). "Modeling of cyclic shear-flexure interaction in reinforced concrete structural walls." *Proc., 15th World Conf. on Earthquake Engineering*, Lisbon, Portugal.

Kolozvari, K., Tran, T., Wallace, J. W., and Orakcal, K. (2014). "Modeling of cyclic shear-flexure interaction in reinforced concrete structural walls—Part II: Experimental validation." *J. Struct. Eng.*, 10.1061/(ASCE)ST.1943-541X.0001083, 04014136.

Lowes, N. L., Lehman, E. D., Birely, C. A., Kuchma, A. D., Marley, P. K., and Hart, R. C. (2012). "Earthquake response of slender planar concrete walls with modern detailing." *Eng. Struct.*, 43, 31–47.

Mansour, M. Y., Hsu, T. C., and Lee, J. Y. (2002). "Pinching effect in hysteretic loops of R/C shear elements." *ACI Spec. Publ.*, 205, 293–321.

Massone, L. M., Orakcal, K., and Wallace, J. W. (2006). "Shear-flexure interaction for structural walls." *ACI special publication SP-236-07—Deformation capacity and shear strength of reinforced concrete members under cyclic loading*, Vol. 236, 127–150.

Massone, L. M., Orakcal, K., and Wallace, J. W. (2009). "Modeling of squat structural walls controlled by shear." *ACI Struct. J.*, 106(5), 646–655.

Massone, L. M., and Wallace, J. W. (2004). "Load—Deformation responses of slender reinforced concrete walls." *ACI Struct. J.*, 101(1), 103–113.

Matlab [Computer software]. Math-Works, Natick, MA.

McKenna, F., Fenves, G. L., Scott, M. H., and Jeremic, B. (2000). "Open system for earthquake engineering simulation (OpenSees)." Pacific Earthquake Engineering Research Center, Univ. of California, Berkeley, CA.

Menegotto, M., and Pinto, E. (1973). "Method of analysis for cyclically loaded reinforced concrete plane frames including changes in geometry and non-elastic behavior of elements under combined normal force and bending." *Proc., IABSE Symp. on Resistance and Ultimate Deformability of Structures Acted on by Well-Defined Repeated Loads*, IABSE, ETH Zurich, Zurich, Switzerland, 15–22.

Oesterle, R. G., Aristizabal-Ochoa, J. D., Fiorato, A. E., Russell, H. G., and Corley, W. G. (1979). "Earthquake resistant structural walls—Tests of isolated walls—Phase II." *Rep. to National Science Foundation*, PCA Construction Technology Laboratories, Skokie, IL, 332.

Oesterle, R. G., Fiorato, A. E., Johal, L. S., Carpenter, J. E., Russell, H. G., and Corley, W. G. (1976). "Earthquake resistant structural walls—Tests of isolated walls." *Rep. to National Science Foundation*, PCA Construction Technology Laboratories, Skokie, IL, 317.

Orakcal, K. (2004). "Nonlinear modeling and analysis of slender reinforced concrete walls." Ph.D. dissertation, Dept. of Civil and Environmental Engineering, Univ. of California, Los Angeles.

Orakcal, K., Ulugtekin, D., and Massone, L. M. (2012). "Constitutive modeling of reinforced concrete panel behavior under cyclic loading." *Proc., 15th World Conf. on Earthquake Engineering*, Lisbon, Portugal.

Orakcal, K., and Wallace, J. W. (2006). "Flexural modeling of reinforced concrete walls—Experimental verification." *ACI Struct. J.*, 103(2), 196–206.

Orakcal, K., Wallace, J. W., and Conte, J. P. (2004). "Flexural modeling of reinforced concrete walls—Model attributes." *ACI Struct. J.*, 101(5), 688–699.

Panagiotou, M., Restrepo, J., Schoettler, M., and Geonwoo, K. (2011). "Nonlinear cyclic model for reinforced concrete walls." *ACI Struct. Mater. J.*, 109(2), 205–214.

Pang, X. D., and Hsu, T. T. C. (1995). "Behavior of reinforced concrete membrane elements in shear." *ACI Struct. J.*, 92(6), 665–679.

Perform-3D [Computer software]. Computers and Structures, Berkeley, CA.

Petrangeli, M., Pinto, P. E., and Ciampi, V. (1999). "Fiber element for cyclic bending and shear of RC structures. I: Theory." *J. Eng. Mech.*, 10.1061/(ASCE)0733-9399(1999)125:9(994), 994–1001.

Ramirez, J. A., and Breen, J. E. (1991). "Evaluation of a modified truss-model approach for beams in shear." *ACI Struct. J.*, 88(5), 562–571.

Sayre, B. (2003). "Performance evaluation of steel reinforced shear walls." M.S. thesis, Univ. of California, Los Angeles.

Scott, R. M., Mander, J. B., and Bracci, J. M. (2012a). "Compatibility strut-and-tie modeling: Part I—Formulation." *ACI Struct. J.*, 109(5), 635–644.

Scott, R. M., Mander, J. B., and Bracci, J. M. (2012b). "Compatibility strut-and-tie modeling: Part I—Implementation." *ACI Struct. J.*, 109(5), 645–654.

Stevens, N. J., Uzumeri, M., and Collins, M. P. (1991). "Reinforced concrete subjected to reversed cyclic shear-experiments and constitutive model." *ACI Struct. J.*, 88(2), 135–146.

Thomsen, J. H., and Wallace, J. W. (2004). "Displacement-based design procedures for slender reinforced concrete structural walls—Experimental verification." *J. Struct. Eng.*, 10.1061/(ASCE)0733-9445(2004)130:4(618), 618–630.

Tran, A. T. (2012). "Experimental and analytical studies of moderate aspect ratio reinforced concrete structural walls." Ph.D. dissertation, Univ. of California, Los Angeles.

Tran, A. T., and Wallace, J. W. (2012). "Experimental study of nonlinear flexural and shear deformations of reinforced concrete structural walls." *Proc., 15th World Conf. on Earthquake Engineering*, Lisbon, Portugal.

Ulugtekin, D. (2010). "Analytical modeling of reinforced concrete panel elements under reversed cyclic loadings." M.S. thesis, Bogazici Univ., Istanbul, Turkey.

Vallenas, J. M., Bertero, V. V., and Popov, E. P. (1979). "Hysteretic behaviour of reinforced concrete structural walls." *Rep. No. UBC/EERC-79/20*, Univ. of California, Berkeley, CA, 234.

Vecchio, F. J., and Collins, M. P. (1986). "The modified compression field theory for reinforced concrete elements subjected to shear." *ACI J.*, 83(2), 219–231.

Vecchio, F. J., and Collins, M. P. (1993). "Compression response of cracked reinforced concrete." *J. Struct. Eng.*, 10.1061/(ASCE)0733-9445(1993)119:12(3590), 3590–3610.

Vecchio, F. J., and Lai, D. (2004). "Crack shear-slip in reinforced concrete elements." *J. Adv. Concr. Technol.*, 2(3), 289–300.

Vulcano, A. (1992). "Macroscopic modeling for nonlinear analysis of RC structural walls." *Nonlinear seismic analysis of RC buildings*, H. Krawinkler and P. Fajfar, eds., Elsevier Science, London, 181–190.

Vulcano, A., and Bertero, V. V. (1987). "Analytical models for predicting the lateral response of RC shear walls: Evaluation of their reliability." *EERC Rep. No. UCB/EERC-87/19*, Earthquake Engineering Research Center, Univ. of California, Berkeley, CA.

Vulcano, A., Bertero, V. V., and Colotti, V. (1988). "Analytical modeling of RC structural walls." *Proc., 9th World Conf. on Earthquake Engineering*, Tokyo, Japan, Vol. 6, 41–46.

Wang, T. Y., Bertero, V. V., and Popov, E. P. (1975). "Hysteretic behaviour of reinforced concrete framed walls." *Rep. No. UBC/EERC-75/23*, Univ. of California, Berkeley, CA, 367.